Int. J. Heat Mass Transfer. Vol. 10, pp. 1618–1622. Pergamon Press Ltd. 1967. Printed in Great Britain

DIFFUSION THERMO EFFECTS IN TURBULENT MASS TRANSFER

C. J. SCOTT* and V. K. JONSSON†

(*Received* 18 *October* 1966 *and in revised form* 12 *May* 1967)

THE PURPOSE of this note is to present Stanton number, recovery factor, and skin friction results for the steady, turbulent, helium–air boundary layer on a flat plate oriented parallel to the freestream flow.

In binary gas mixtures the lighter-weight component will migrate toward the warmer region and the heavier toward the cooler. This phenomenon, known jointly as thermal diffusion or the Soret effect, and its converse, diffusion thermo or the Dufour effect, are not new—having been discovered in 1856 and 1873, respectively. Essentially thermal diffusion is a diffusive mass flux due to a temperature gradient while diffusion thermo is an energy flux due to concentration gradient. The two diffusional processes are thermodynamically coupled phenomena and occur simultaneously in a multi-component flow.

Pertinent experimental and analytical studies of the laminar boundary layer with these diffusional processes are summarized in [1, 2] for both forced and free convective flows. Also included in [1] is a detailed analysis aimed at clarifying the relative importance of thermal diffusion and diffusion thermo on the heat transfer and skin friction for the several flows. It has been established that experimentally observed adiabatic wall temperature trends with gas injection were due entirely to diffusion thermo, with thermal diffusion playing only a secondary role.

The early analysis of Rubesin and Pappas [3] on the turbulent binary boundary layer contains neither a Mach number effect nor the thermal diffusion combination. Culick [4] made order of magnitude estimates of thermal diffusion effects using a perturbation scheme to demonstrate that the adiabatic wall temperature is more dependent on thermal diffusion than is the heat-transfer coefficient. Culick's work suffers from the unnecessary assumptions of a Schmidt number of unity in the sublayer and both Prandtl and Schmidt numbers unity in the turbulent zone. Later, Ness [5] improved these property assumptions while omitting the thermal diffusion combination. The present work [6] extends the analysis of Ness by including diffusion thermo in the sublayer. According to the laminar results referred to above, thermal diffusion is ignored. No turbulent analogue to diffusion thermo is considered [7].

Three key assumptions are made in the present analysis:

1. The boundary layer is divided into two regions—i.e. a thin laminar sublayer close to the wall in which the molecular property values appear alone in the transport equations; and a much thicker turbulent outer region away from the wall where the molecular transport coefficients are neglected with respect to the eddy diffusivities. The velocity, temperature, concentration, shear, and total energy fluxes are continuous at the interface of the two layers.
2. In the transport equations, variations of the velocity, temperature, or concentration with streamwise coordinate are assumed negligible compared to variations with respect to normal coordinate. This second assumption, which replaces the partial differential equation by more easily solved total differential equations, has led to useful results when applied to the low speed problem. The variations in the streamwise x-direction are ultimately introduced by the x-variation of the wall shear as determined from the Von Kármán momentum integral equation.
3. On the basis of comparable laminar flow solutions, thermal diffusion is neglected in both the sublayer and outer layer and diffusion thermo is included only on a molecular basis. The numerical results are restricted to the case of helium blowing into an airstream.

For a given problem the freestream Mach number, M_δ, and the injection parameter, $\zeta = 2(\rho_w v_w)/(\rho_\delta U_\delta)(C_f)$, were prescribed along with the wall-to-freestream temperature ratio, T_w/T_δ. Foreign gas mass concentration, C_1, is the basic independent variable and the interface (subscript a) concentration C_{1a} is of primary importance. In the sublayer $C_{1w} \geqslant C_1 \geqslant C_{1a}$, while the outer layer $C_{1a} \geqslant C_1 \geqslant C_{1\delta} = 0$. The starting profile at x_0 is obtained by setting $C_{1a} = 0$ which corresponds to the initial profile. An example of the initial profile is given in Fig. 1 which illustrates the development of the turbulent velocity profile from an initially "laminar-like" profile. The initial profile is universal such that the final results do not contain dependences on R_{x_0}. For larger

* Associate Professor of Mechanical Engineering, University of Minnesota.

† Lecturer in Mechanical Engineering, Imperial College of London.

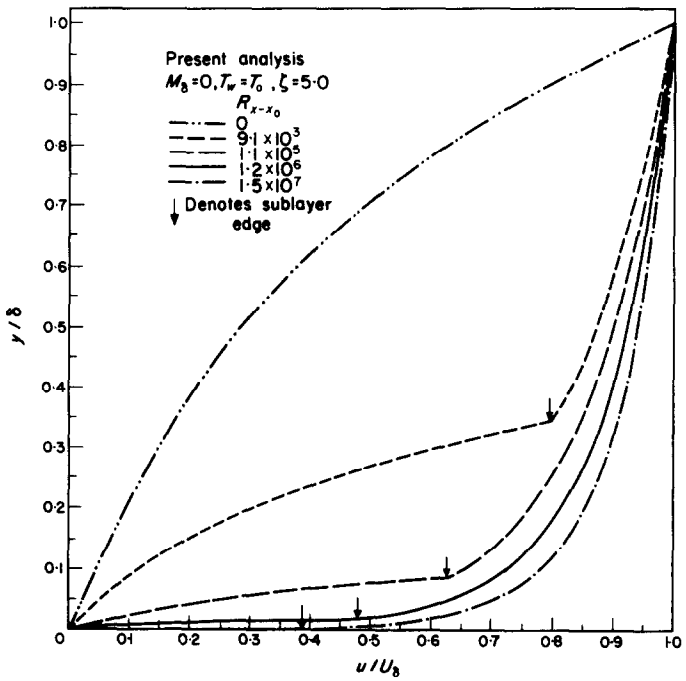

FIG. 1. The development of turbulent velocity profile from an initially laminar profile.

values of x, C_{1a} increases and approaches C_{1w}. Correspondingly the interface velocity decreases from the free-stream velocity and approaches zero at large Reynolds number (x).

A total of 100 y-locations (or better local concentrations) were used—divided equally between the sublayer and outer layer. Fifty x-locations (or better interface concentrations) were used resulting in a single solution which consists of 100 point profiles at 50 stations. The use of a digital computer to develop step-by-step solutions requires some justification here because of the acknowledged lack of precision in the turbulence assumptions. Historically, in the far simpler air–air problem, the commonly employed assumptions of both laminar and turbulent Prandtl numbers equalling unity results in a known relation between temperature and velocity such that the energy equation need not be solved. A combination of the momentum and continuity equations is solved to yield the velocity distribution with the local wall shear as a parameter. The velocity distribution is inserted into the momentum thickness integral. The integral cannot be solved in closed form and frequently approximations such as the first term of a series expansion are used which are valid only for small values of the wall shear and injection rate. The Von Kármán momentum integral equation is then integrated using the approximate $C_f(Re_\theta)$ relation to produce the desired variation of local skin friction with Re_x. Again the integration cannot be made in closed form and the method of evaluating the quadrature often is to use the first term of a series expansion.

The extension of the problem to include foreign gas injection introduces a species mass conservation equation and another property dependence. Only numerical integration schemes are capable of handling the variations of the properties with both concentration and temperature. Effects such as diffusion thermo add new terms to the integrands of the quadratures to further complicate the integrations. A scrupulous insistence on "more exact" integrations can be justified here since we are concerned with demonstrating the relative small effects of diffusion thermo.*

The numerical comparisons presented in Figs. 1–6 are, for space purposes, confined mainly to a freestream Mach number M_δ of 4·0. Solutions including diffusion thermo involve a non-zero thermal diffusion factor α while diffusion thermo is suppressed in the calculations when $\alpha = 0$. The thermal diffusion factor was held constant at a given injection rate while allowed to vary with injection rate. The numerical value was determined from the average level of

* Complete derivations and extensive numerical results are given in [6].

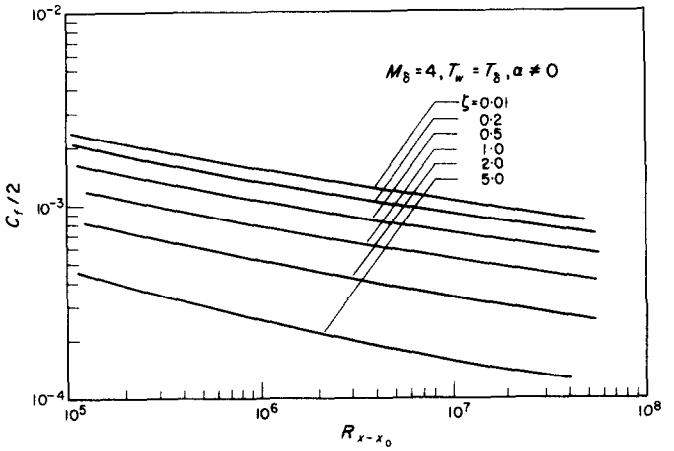

FIG. 2. Local skin friction coefficients with helium injection.

concentration in the sublayer according to the relation $\alpha = -0{\cdot}2 - 0{\cdot}5(C_{1w} + C_{1\delta})/2$. Values of the local skin friction coefficient vs. Reynolds number are presented in Fig. 2 while the normally observed reductions in skin friction with helium injection are presented in Fig. 3.

The surface heat flux is written:

$$Q_w = -k\frac{\partial T}{\partial y}\bigg]_w + \rho_w v_w C_{p1} T_w + \rho_w v_w (1 - C_{1w})\alpha \frac{M_w^2}{M_1 M_2} R_w T_w. \quad (1)$$

The term $\rho_w v_w C_{p1} T_w$ is the injected enthalpy flux. The term need not be included in a presentation of analytical results since, in application, it can be properly included in the appropriate energy balance. The remaining energy transfer arises from thermal conduction and diffusion thermo

$$Q_{wc} = -k\frac{\partial T}{\partial y}\bigg]_w + \rho_w v_w (1 - C_{1w})\alpha \frac{M_w^2}{M_1 M_2} R_w T_w. \quad (2)$$

In Fig. 4, Q_{wc} is made dimensionless by means of the freestream enthalpy flux $\rho_\delta U_\delta h_\delta$. Results are given for wall temperatures equalling the freestream static (T_δ) and freestream stagnation ($T_{0\delta}$) temperatures. For a cooled wall ($T_w = T_\delta$), the lower portion of Fig. 4 reveals that diffusion thermo increases the surface heat flux at all Reynolds numbers and injection rates—a result anticipated from equation (2) where the two terms are additive since α is negative for light gas injection. The heat flux increment due to diffusion thermo, represented by the vertical distance between the two curves, ultimately decreases with increased injection because of the increase in wall concentration [$(1 - C_{1w})$ term in equation (2)]. The decrease in wall heat flux with increased injection is apparent at all Reynolds numbers.

The stagnation temperature results, ($T_w = T_{0\delta}$, actually a slightly heated wall), are rather mixed. In this case the conductive and diffusion thermo terms are of opposite sign and are relatively equal in magnitude. The Reynolds number dependence of the two effects is quite different—

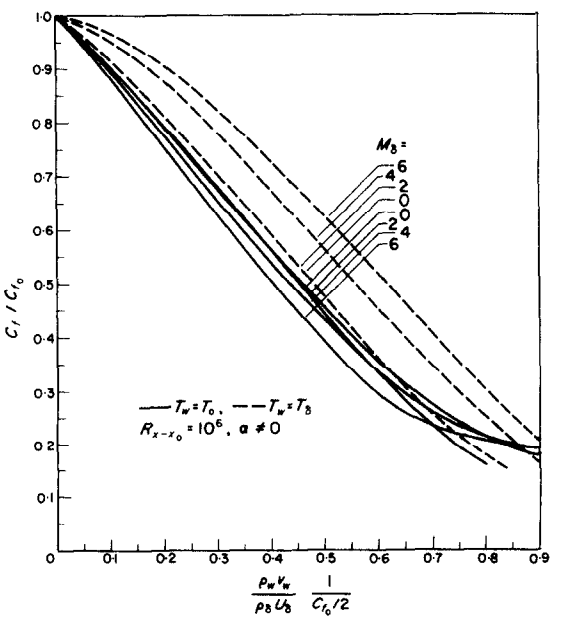

FIG. 3. The reduction in skin friction with helium injection—turbulent boundary layer.

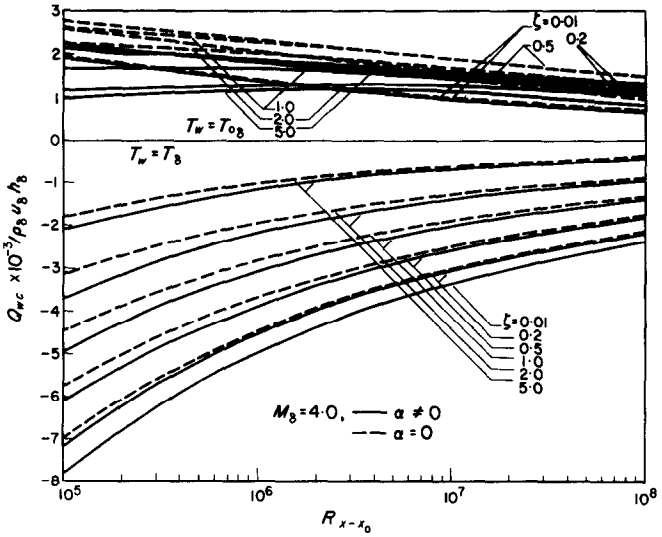

FIG. 4. The effect of diffusion-thermo on local energy transfer rates.

actually opposite trends are evident at the larger injection rates. At intermediate injection rates the heat flux is nearly independent of Reynolds number while at near-zero injection rates the heat flux decreases with Reynolds number in the normal fashion.

The adiabatic wall case is defined by the condition $Q_{wc} = 0$ in equation (2). The surface temperature for this condition is the adiabatic wall temperature (T_{aw}). In view of the strong Reynolds number dependence of the heat flux in Fig. 1, the adiabatic wall temperature also proves to be Reynolds number dependent. Special techniques are required to determine T_{aw} since the adiabatic condition is attained only at one point along the wall. Since there is a lack of universality concerning the adiabatic condition, no special search routines were developed. The problem was avoided by definition of a heat-transfer Stanton number, St, which is independent of temperature ratio (1).

$$St = \frac{Q_{wc}}{\rho_\delta U_\delta C p_\delta (T_w - T_{aw})}. \tag{3}$$

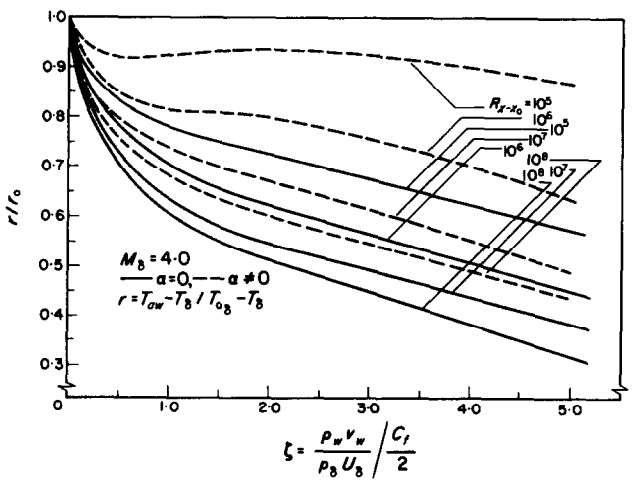

FIG. 5. The reduction in temperature recovery factor with helium injection—turbulent boundary layer.

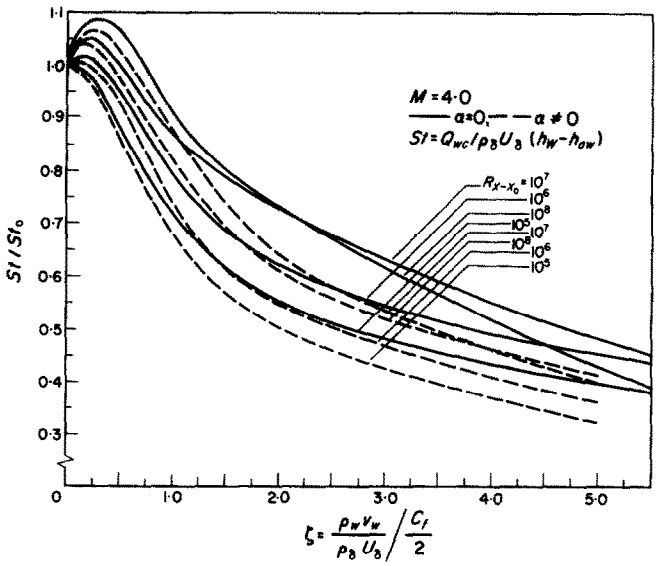

FIG. 6. The reduction in heat-transfer parameter with helium injection—turbulent boundary layer.

The adiabatic wall temperatures, $T_{aw}(Q_{wc} = 0)$, were obtained by a linear interpolation between $Q_{wc}(T_w = T_\delta)$ and $Q_{wc}(T_w = T_{0_\delta})$. The temperature recovery factors, as defined by the relation $r = (T_{aw} - T_\delta)/(T_{0\delta} - T_\delta)$ are given in Fig. 5. There is a general tendency for the recovery factor to decrease with increasing rates of injection, although diffusion thermo diminishes the trend considerably.

The heat-transfer Stanton numbers are given in Fig. 6. The effect of small amounts of helium injection is first to slightly increase the Stanton number. At low injection rates the resistance to heat flow is predominantly laminar and proportional to the local Prandtl number near the wall. For helium–air mixtures the Prandtl number is known to undergo an initial decrease with concentration and finally an increase. With Fig. 6 in mind, caution must be exercised in extrapolating Stanton number measurements to obtain zero injection values. At intermediate injection rates diffusion thermo decreases the Stanton numbers. At low injection rates the variation of St with Reynolds number is opposite that of (3) and is due to the initial laminar boundary layer. At the largest injection rates the usual Reynolds number dependence is beginning to appear.

REFERENCES

1. E. M. SPARROW, W. J. MINKOWYCZ and E. R. G. ECKERT, Diffusion-thermo effects in stagnation-point flow of air with injection of various molecular weights into the boundary layer, *AIAA Jl* **2**, 652–659 (1964).
2. J. R. BARON, Thermodynamic coupling in boundary layers, *ARS Jl* **32**, 1053–1059 (1962).
3. M. W. RUBESIN and C. C. PAPPAS, An analysis of the turbulent boundary layer characteristics on a flat plate with distributed light gas injection, NACA TN 4149 (February 1962).
4. F. E. C. CULICK, The compressible turbulent boundary layer with surface mass transfer, MIT Naval Supersonic Laboratory TR 454 (August 1960).
5. N. NESS, Foreign gas injection into a compressible turbulent boundary layer on a flat plate, General Electric Space Sciences Laboratory Report R60SD410 (August 1960).
6. C. J. SCOTT and V. K. JONSSON, Thermal diffusion effects in turbulent mass transfer, Heat Transfer Laboratory TR 66. Department of Mechanical Engineering, University of Minnesota (October 1965).
7. H. THOMANN and J. R. BARON, Experimental investigations of thermal diffusion effects in laminar and turbulent shear flow, *Int. J. Heat Mass Transfer* **8**, 455–466 (1965).